EMPIRICALLY MODELING HYPERVELOCITY SABOT SEPARATION

An Undergraduate Research Scholars Thesis

by

JAMES LEAVERTON

Submitted to the LAUNCH: Undergraduate Research office at
Texas A&M University
in partial fulfillment of requirements for the designation as an

UNDERGRADUATE RESEARCH SCHOLAR

Approved by
Faculty Research Advisor: Dr. Thomas E. Lacy, Jr.

May 2021

Major: Mechanical Engineering

RESEARCH COMPLIANCE CERTIFICATION

Research activities involving the use of human subjects, vertebrate animals, and/or biohazards must be reviewed and approved by the appropriate Texas A&M University regulatory research committee (i.e., IRB, IACUC, IBC) before the activity can commence. This requirement applies to activities conducted at Texas A&M and to activities conducted at non-Texas A&M facilities or institutions. In both cases, students are responsible for working with the relevant Texas A&M research compliance program to ensure and document that all Texas A&M compliance obligations are met before the study begins.

I, James Leaverton, certify that all research compliance requirements related to this Undergraduate Research Scholars thesis have been addressed with my Research Faculty Advisor prior to the collection of any data used in this final thesis submission.

This project did not require approval from the Texas A&M University Research Compliance & Biosafety office.

TABLE OF CONTENTS

Page

ABSTRACT

Empirically Modeling Hypervelocity Sabot Separation

James Leaverton
Department of Mechanical Engineering
Texas A&M University

Research Faculty Advisor: Dr. Thomas E. Lacy, Jr.
Department of Mechanical Engineering
Texas A&M University

The aerodynamic sabot discard process is crucial to the success of hypervelocity testing using less than ideal projectile launch properties or sub-caliber projectiles in smooth bore launchers. Achieving efficient sabot separation is integral to both reaching extreme velocities and capturing distinguishable impact phenomena during testing. In this study, the conical-cup discard technique is investigated for four-petal sabot packages carrying 2-8 mm diameter spherical projectiles launched with the state-of-the-art 2-stage light gas gun located in the Texas A&M University Hypervelocity Impact Laboratory. Image processing techniques are employed to convert images of sabot petal impacts to coordinate entities. The degree of separation for each entity is then characterized by the distance travelled in the radial direction away from the projectile's nominal launch trajectory. An empirical model relating both environmental and launch parameters to the degree of sabot separation at a fixed distance from the muzzle is developed using polynomial regression. Projectile velocity, nitrogen atmosphere backfill pressure, and sabot geometry are found to be significant regressors in predicting the degree of

separation. Additional analysis is conducted to qualitatively understand the model in the context of test results and aerodynamic laws.

DEDICATION

For Mike.

ACKNOWLEDGEMENTS

Contributors

I would like to thank my faculty advisor, Dr. Lacy for providing me every resource I needed to succeed: not just in this study, but throughout my entire tenure in the Hypervelocity Impact Lab.

I would also like to thank Dr. Raj Kota, Jacob Rogers, Paul Mead, Aniket Mote, and all my other colleagues in the Hypervelocity Impact Lab for their continued guidance and support. I am especially grateful to Paul Mead for his help in the data collection for this project.

Finally, thanks to Zach Wantz of Physics Applications Inc. for his ideas and help in the creation of this project.

All hypervelocity empirical data used in this thesis is sourced from the Hypervelocity Impact Lab's 2-stage light gas gun located at the Center for Infrastructure Renewal on Texas A&M University's RELLIS campus.

All other work conducted for the thesis was completed by the student independently.

Funding Sources

Undergraduate research through the Hypervelocity Impact Laboratory was supported by the U.S. Army Futures Command through the cooperative agreement between Texas A&M University and the Army Research Laboratory. No other funding contributions were used for this research.

1. INTRODUCTION

Recent developments in hypersonic capabilities by the United States' foreign adversaries [1], along with the increasing amount of man-made orbital debris (MMOD) [6], are creating a demand in the scientific community for hypervelocity impact (HVI) investigations. Hypervelocity impact occurs when a projectile with a relative velocity greatly exceeding the standard temperature and pressure speed of sound (commonly defined as greater than Mach 5 or ~2000 m/s) [2], impacts a material or structure. Defending against these HVIs is crucial as even microscopic projectiles traveling at hypervelocity pose a serious threat [3-6]. Due to these threats, developing structural materials to protect against HVIs is vital to the security of our nation.

The Hypervelocity Impact Laboratory (HVIL) at Texas A&M University conducts research to enable unique high strain-rate materials characterization along with multiscale numerical model development and implementation. The HVIL features a robust testbed for the development and testing of materials to mitigate HVIs. Experiments are conducted using a state-of-the-art 2-stage light gas gun (2SLGG) capable of launching 2-10 mm diameter projectiles at velocities in the range of 2-8 km/s. The 2SLGG is equipped with a high-speed camera capable of filming up to 10 million frames per second, as well as other diagnostic equipment such as a flash X-Ray system, a high-speed thermal imaging camera, an AMOtronics Transient Recorder system, and a photon Doppler velocimetry system. This highly capable in-situ diagnostic setup allows for the comprehensive study of hypervelocity impact phenomena.

Achieving hypervelocity with an increasing projectile mass is a considerable feat. The 2SLGG, shown in Figure 1.1, accelerates projectiles in two stages: first, a firing system ignites a primary charge in the firing breech, located at the most uprange point. This charge in turn lights the secondary charge, whose mass serves as the 2SLGG's primary performance variable. The resulting expanding gas forces a polymer piston downrange through the pump tube. This piston compresses a light gas, typically hydrogen. The gas is compressed into the central breech, which hydraulically separates the high-pressure pump tube (first stage) from the evacuated launch tube, blast tank, and target tank (second stage) via a petal valve (i.e., pressure disk). Upon reaching a critical pressure, the petal valve ruptures, freeing the high-pressure working gas into the launch tube and thus rapidly accelerating the projectile package downrange towards the blast tank (Figure 1.1). Before each hypervelocity test, the blast tank is vacated of air with a vacuum pump. Then, 0.1 – 0.35 atm of nitrogen is introduced to form a low-density atmosphere for the projectile package to travel through. This introduced nitrogen is referred to as backfill.

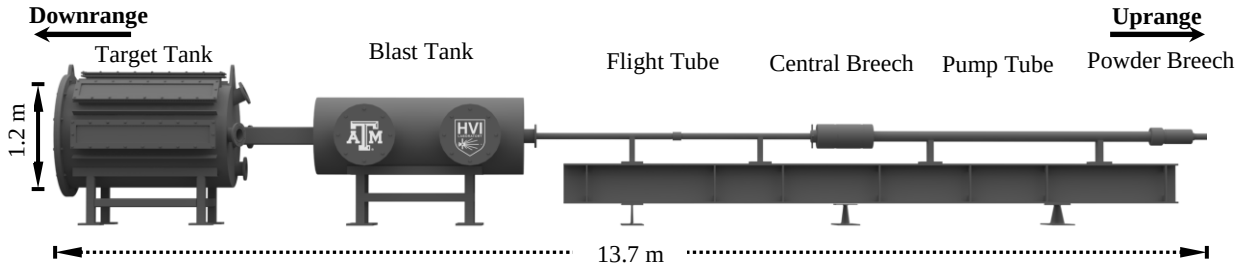

Figure 1.1. 3D render of the Texas A&M University Hypervelocity Laboratory's 2-stage light gas gun.

The 2SLGG features a smooth-bore launch tube that allows multiple size projectiles to be launched using a projectile package. The projectile package is commonly referred to as a sabot package, or sabot and projectile. The sabot package provides projectile stability through its acceleration down the flight tube of the 2SLGG. The sabot is usually formed with three or four 'petals' that surround the projectile while fitting flush inside the launch tube. A package with the equivalent caliber as the flight tube is crucial to achieving the desired hypervelocity by ensuring

a tight seal between the inside of the bore and the package, which guarantees efficient transfer of energy from the expanding gas to the projectile package [8].

After accelerating down the flight tube, the sabot package must be separated from the projectile. Projectiles travelling at hypervelocity in atmosphere require a low-drag configuration to preserve kinetic energy [9]. Additionally, in hypervelocity testing, projectile mass is measured to understand the energy transfer to the target on impact [10]. For these reasons, the sabot must be discarded before the projectile impacts any target. Various methods are used in both hypervelocity testing and real-world hypersonics applications to achieve this sabot separation [9]. Spin separating sabots use angular velocities achieved through a rifled bore to separate the sabot petals while allowing the projectile payload to continue traveling on its nominal launch trajectory. This method has limitations, as the bore of the launch tube must be manufactured with a low-pitch rifling to both rotate the sabot package and protect against stripping of the rifling from repeated firing.

A more common sabot separation configuration in hypervelocity testing is aerodynamic separation [8, 9]. The HVIL's 2SLGG uses aerodynamic separation for hypervelocity testing. A typical aerodynamically separating sabot is a nylon right circular cylinder separated into three or four azimuthal sections, or petals, that enclose the projectile at the downrange edge. The projectile fits in a machined spherical cup that is formed when the four sabot petals are assembled. On the inside surface of each petal, angled v-notches that fit together transmit the accelerating forces through all four petals. The outer diameter of the sabot package is machined to sit flush inside the bore of the launch tube. Sabot packages are designed with a cup-like indention on the forward-facing edge to induce separation. When the package exits the launch tube after accelerating, ram pressure from the sabot travelling through atmosphere produces a

resultant aerodynamic force and moment on the sabot petals causing them to separate radially outward from the axis of penetration and fall away (Figure 1.3). The amount of atmosphere that the sabot flies through determines the degree of separation. In the HVIL, the sabot package is separated by the nitrogen backfill in the blast tank. Figure 1.2 shows an aerodynamically separating sabot machined for a 6 mm spherical projectile.

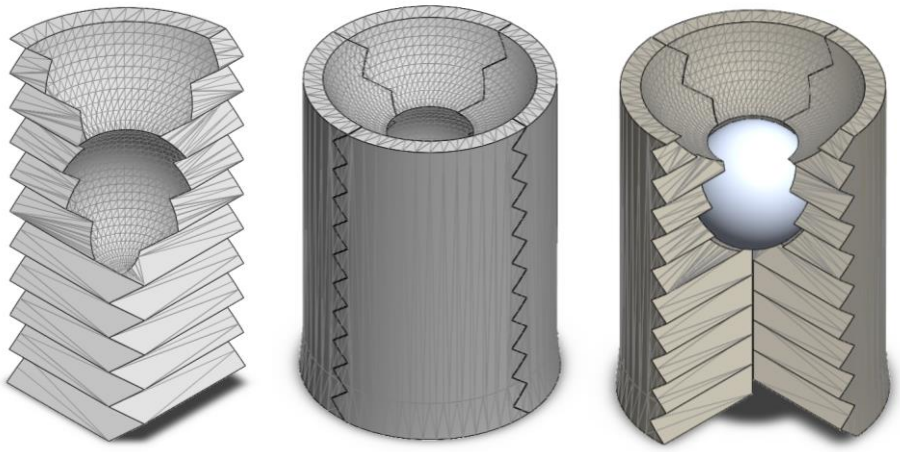

(a) (b) (c)

Figure 1.2. Nylon cylindrical sabot machined for 6 mm spherical projectile: (a) single azimuthal sabot petal, (b) sabot package with four azimutal petals assembled without projectile, (c) sabot package displaying inserted spherical projectile with one azimuthal section removed.

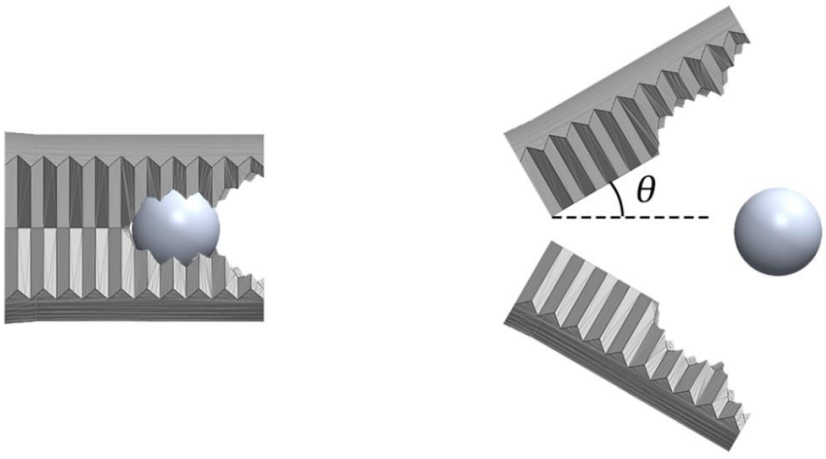

(a) (b)

Figure 1.3. Rendition of sabot in flight with the horizontal petals removed: (a) the sabot package's position the instant it exits the launch tube, (b) the sabot package's position sometime later in flight. The sabot petals are peeled away from the nominal projectile flight path, while also slowing down relative to the projectile from aerodynamic drag forces. A sabot petal's angle of rotation with respect to the projectile's nominal flight path is denoted as theta.

Historically, sabot separation characterization has been conducted through trial-and-error processes for individual 2SLGGs. Unique launching requirements and the nature of extreme launching performance prompt specialized, diagnostic, iterative design for each hypervelocity testing configuration. Attempts have been made to empirically model sabot flight and impact properties. Grosch et al. (1993) have observed an empirical relationship between sabot separation and flight chamber pressure (2 – 16 torr) for a constant velocity. These tests were conducted using two-piece 1.78 mm diameter nylon lexan sabots.

Swift et al. (1987) introduced a straightforward, analytical method to approximate sabot separation utilizing the sabot petal's geometry and density, as well as properties of the atmospheric medium that causes separation. This analysis produced a second order differential equation describing the angular acceleration of the sabot petals as a result of the aerodynamic moment. Integrating this equation yields the angle of rotation between the sabot petal and the nominal projectile flight path as the sabot petal pivots about its rear corner. The angle of rotation is expressed as a function of the distance the package has travelled through atmosphere. Implementing this model gives a relatively effortless estimate of the angle of the sabot at a fixed distance in its flight trajectory (i.e. traveling through the blast tank and impacting the sabot stripper). This model, however, is not completely accurate in describing sabot separation phenomena in the HVIL's 2SLGG. Experimental results from the HVIL show that as the sabot rotates about its rear corner, it also experiences translational motion radially outward, resulting in the degree of separation. The angular acceleration equation neglects the radially outward aerodynamic forces that cause translational movement of the sabot radially away from the nominal projectile flight path.

During the initial testing and calibration of the HVIL's 2SLGG, sufficient sabot separation was achieved through an iterative trial-and-error process of tuning launch parameters. The HVIL team formulated a primitive model to predict sabot separation given these parameters, but there is inherent value in developing an empirical model to accurately predict sabot separation in hypervelocity testing. Efficient sabot separation reduces both testing turnaround time and consumable testing resource expenditure. In the development of new hypervelocity testing facilities, preexisting models are invaluable in the preliminary optimization of any 2SLGG performance, despite the likelihood of varying launch requirements with facility. The present study develops a rigorous empirical model to investigate the effects of launch parameters on the degree of aerodynamic sabot separation for the Texas A&M University Hypervelocity Impact Laboratory's 2-stage light gas gun, with the goal of validating future analytical models utilizing aerodynamic laws.

2. METHODS

2.1 Data Acquisition

To determine the degree of sabot petal separation in the 2SLGG, visual data was acquired through photography of the sabot stripper plate. After aerodynamic separation, sabot petal impacts result in large indentions in the 6-inch diameter steel stripper plate. Throughout the stripper plate's service life, the resulting surface damage compounds to form a cratered surface. To distinguish new impacts, standard operating procedure included painting the face of the sabot stripper with a white primer spray paint. After each hypervelocity test, the stripper plate was inspected and photographed using an iPhone X camera balanced on the baffle in the center of the blast tank and focused on the stripper plate. The phone's camera was positioned so that the central vector of the camera's field of view was coincident with the axis of penetration and normal to the face of the stripper plate (Figure 2.1a). Post-test photography was performed on successful tests, defined as all four sabot petals impacting the stripper plate with no sabot petals entering the target tank and impacting the target.

The raw images were then imported into Adobe Photoshop CC 2015 on a standard canvas size of 2000 by 2000 pixels. The images were scaled to position the outer circumference of the stripper plate concentric with a standard circular outline (diameter of 1836 pixels) centered on the canvas. Three images had not initially been photographed in a configuration coincident with the axis of penetration and were thus adjusted with Photoshop's perspective tool to remove any eccentricity, assuring the sabot stripper plate was normal to the camera.

Sabot petal impacts form indentations 0.15 – 0.75 in. deep dependent on the grade of steel and impact velocity. Over time, the steel stripper plate is deformed until it is no longer

effective and must be replaced. These indentions expose new steel not coated in the white paint; the contrast of the exposed steel with the white paint permits easier identification of the impact location. These impact locations were traced and converted into black entities in Photoshop. As shown in Figure 2.1b, these entities were exported with a white background to form a black and white vector image.

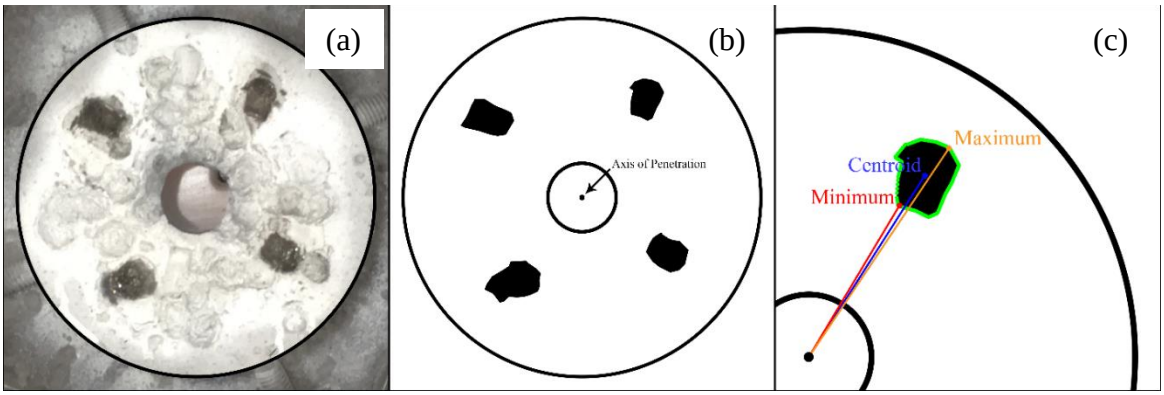

Figure 2.1. Data collection and processing: (a) example photograph of the impacted sabot stripper plate, (b) same photograph traced and converted to binary image, (c) calculated centroid, min, max distances for an impact contour

To quantify the degree of sabot separation, the radial distance between each impact and the axis of penetration was measured. To convert the visual data into measurable quantities, edge detection software was developed in Python using the Open Source Computer Vision Library (OpenCV). The vector images were imported into the script and converted to greyscale, transforming the RGB channels into a single channel with each pixel being assigned an intensity value ranging from 0 (black) to 255 (white). Each greyscale image was then converted to a binary image using OpenCV's threshold function, using the 50% grey value of 127. From this binary image data, the sabot petal impact entities were converted into contours using OpenCV.

In OpenCV, contours were identified by a curve joining all the continuous points along the boundary of an entity possessing the same color or intensity. A boundary with edge points was fitted to each impact entity, with X and Y pixel positions assigned to each edge point. For

each image, the software iterated through each of the four sabot petal impact contours and found the two-dimensional Euclidean distance in pixels between each edge point and the axis of projectile penetration (Figure 2.1c). The distance between the closest and farthest edge points from the axis of penetration was recorded to characterize the degree of separation in the radial direction.

Additionally, the centroid, or geometric center, of each contour was found using OpenCV's Image Moment function. Image Moment uses a weighted average of pixel intensities to calculate the centroid. Each sabot petal impact entity had a uniform intensity, effectively implementing the arithmetic mean position of all points in a shape. The Euclidean distance between each contour's centroid and the axis of penetration was calculated. For each sabot stripper image, the contours' four centroid distances were averaged. The minimum and maximum distances were also averaged to respective values. All distances were then converted from pixels into inches. Values of the degree of separation were collected for 35 hypervelocity tests. Tests utilizing sabots machined to launch 4 mm and 10 mm spherical projectiles were studied.

The sabot strike contour circularity, or the measure of how closely the shape of an object approaches a perfect circle, was of particular interest. In digital image processing, circularity is commonly defined by Equation 2.1. For circles, this ratio is equal to 1; for non-circles, the ratio is greater than one. The circularity was calculated for each impact contour using OpenCV's perimeter and area functions. For each test, the circularity values of the four impact contours were averaged and recorded along with the test velocity.

$$Circularity = \frac{Perimeter^2}{4 \cdot \pi \cdot Area} \tag{2.1}$$

2.2 Statistical Analysis

A statistical approach was chosen to develop the empirical model predicting the degree of sabot separation. Along with the acquired degree of separation data, recorded testing parameters were selected for polynomial regression. Launch parameters, such as projectile velocity (ranging from 2000 to 7000 meters per second) and target tank backfill pressure (90 – 250 Torr) were considered for independent variables in the model. Additionally, a binary variable was introduced to the polynomial regression to distinguish the testing sabot geometry between the 4 mm and 10 mm sabots. The 10 mm sabot features a larger quarter-sphere cup to hold the 10 mm diameter projectile. The spherical cup increases the surface area of the projected area normal to the freestream velocity in early separation. This negative space also reduces the mass and decreases the local moment of inertia at the downrange part of the sabot petal. This reduced moment of inertia produces less resistance to early rotation in the separation process.

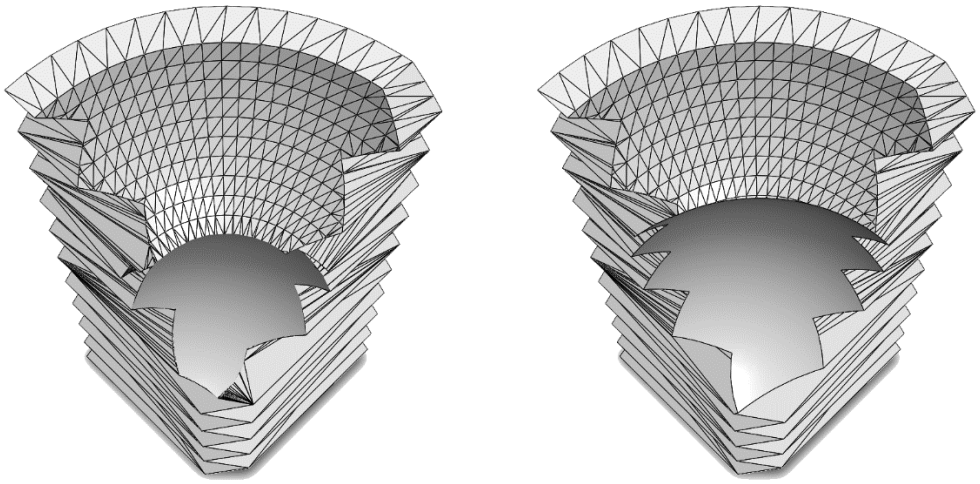

Figure 2.2. Projected area as viewed from a 25° angle. This view shows the leading edge of a single sabot petal as it flies headlong into the freestream velocity: (a) a sabot petal machined for a 6 mm projectile (b) a sabot petal machined for a 10 mm projectile. Each petal has already rotated $\theta = 25°$ away from the projectile's nominal flight trajectory. It is easy to observe the difference in surface area facing normal to the free stream velocity. The 10 mm sabot's larger spherical cup allows more freestream velocity to impart a larger aerodynamic force to assist in separation.

The polynomial regression was constructed employing an understanding of phenomena governed by the laws of aerodynamics. An increase in backfill pressure would entail an increase in the degree of separation [7] due to the increased ram pressure which induces larger magnitude aerodynamic forces that cause separation. Pressure and pressure squared were chosen to be regressors to investigate the effects of pressure on sabot separation were linear or nonlinear in nature. When backfill pressure is present, an increase in velocity would also warrant an increase in degree of separation due to the increased freestream velocity and therefore ram pressure. However, when zero backfill pressure is present and the sabot package is travelling through a true vacuum, a lack of aerodynamic forces in any direction would cause the package to fly true and not separate. Velocity with no interaction term would not accurately describe the sabot separation, as any coefficient would affect the degree of separation even with no backfill pressure. For this reason, velocity was not chosen to be a standalone regressor. All data points collected during hypervelocity testing featured a backfill pressure of at least 90 Torr. As the sabot would not separate to impact the stripper plate with minimal backfill pressure, a degree of separation data point is not measurable with the experimental setup. The HVIL has tested several polymer cylinders over a wide hypervelocity range with backfill pressures approaching 0 Torr. Despite a leading edge normal to the freestream velocity, the cylinders appeared to experience little rotational or translational deviation from the nominal flight trajectory. To account for minimal separation at any velocity with no backfill pressure, a single artificial data point was added to the 35 recorded points in the regression model. The attributes for this data point included a randomized velocity value in the operating range and a backfill pressure value of 0 Torr. A mean imputed value of 0.5 was inputted for the sabot geometry binary variable so the regression would apply the zeroing value for both the 4 mm and 10 mm sabots.

As the sabot would only experience increasing separating forces with increasing velocity when backfill pressure was present, an interaction term between velocity and pressure was chosen to be the final regressor. The regression equation, displayed below, designates velocity as V, backfill pressure as P, and the sabot binary variable as S.

$$\widehat{Degree\ of\ separation} = x_1 P + x_2 VP + x_3 P^2 + \beta_1 S + u \qquad (2.2)$$

3. RESULTS

The polynomial regression model yields an R Square value of 0.92 for the 35 data points. The standard error of 0.11 inches indicates an accurate model for the data provided. All regressors prove to be statistically significant at the p = 0.01 level. The intercept is statistically significant at the p = 0.05 level. As expected, the sabot geometry generates a pronounced effect on the degree of sabot separation. The coefficient indicates that a 10 mm sabot will experience a 0.27 inch increase in degree of separation compared to a 4 mm sabot for a given velocity and backfill pressure. To understand the composition of the degree of separation, an average value within the tested range for each regressor is multiplied by its respective coefficient. Approximate mean values of 4500 meters per second and 150 Torr are used in Table 3.2.

Polynomial Regression Results	
Multiple R	0.961660131
R Square	0.924790208
Adjusted R Square	0.915085718
Standard Error	0.106749989
Observations	36

	Coefficients	*Standard Error*	*t Stat*	*P-value*
Intercept	0.266820563	0.098291366	2.714588	0.010743
Pressure	0.00918261	0.001081598	8.489854	1.37E-09
Velocity · Pressure	4.88406E-07	1.69934E-07	2.874084	0.007257
$Pressure^2$	-1.71064E-05	3.27725E-06	-5.21975	1.14E-05
10 mm Sabot	0.266455432	0.045896694	5.805547	2.14E-06

Table 3.1. Polynomial regression results.

Regressors	*Coefficients*	*Composition (inches)*	*Composition (percent)*
Intercept	0.266820563	0.26682	14.38
Pressure	0.00918261	1.37739	74.24
Velocity · Pressure	4.88406E-07	0.32967	17.77
$Pressure^2$	-1.71064E-05	-0.38489	-20.74
10 mm Sabot	0.266455432	0.26646	14.36
	Sum	1.85545	100.00

Table 3.2. Example of mean parameters inputted into the regression model to predict the degree of sabot separation. Values of 4500 m/s and 150 Torr were used for velocity and pressure, respectively. A 10 mm sabot was considered. These average indicate the composition of the resulting predicted separation in terms of the regression coeffcients.

For reference, a 3D surface showing the polynomial regression results is shown below in Figure 3.1. The surface is generated using a simpler regression model with no geometry distinction; the binary variable indicating a 4 mm or 10 mm sabot is not included in the regression. Data points included in the regression are also plotted. In Figure 3.2, the colormap is visualized on a rendition of the sabot stripper plate. The plate features a 1.25 inch diameter center hole for the projectile to pass through to continue on to the target tank; the outer diameter of the stripper plate is 3 inches. The colormap applied to the surface is depicted on the surface of the stripper plate. The green radial sections indicate a desirable degree of separation. The interior orange radial section indicates a lack of sabot separation, resulting in a sabot strike into the target being tested. The exterior orange radial section demarcates the zone in which the sabot will separate to the edge of the stripper plate. A degree of separation approaching the edge of the sabot stripper plate is not desirable. Velocity and backfill pressures required to obtain these values often introduce aerodynamic heating to the projectile just before target impact. The aerodynamic heating manifests as a bright flash in the high-speed camera, restricting observation of projectile impact. Over-separation further risks impacting the interior surface of the blast tank.

Even still, high velocity and backfill pressure combinations can generate aerodynamic forces large enough to cause the sabot to fail. When sabot petals fail in testing, the fractured pieces do not separate and impact the target. To minimize the risk of sabot failure, the preferable degree of separation lies in a range of 1 – 2 inches.

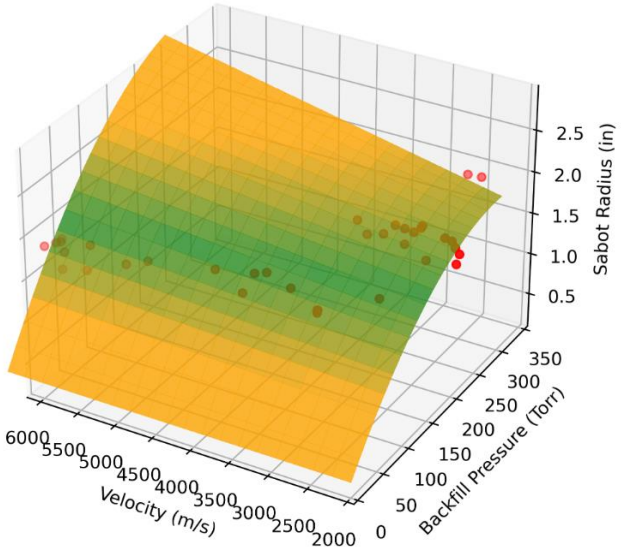

Figure 3.1. 3D surface of the degree of separation. Sabot geometry is not distinguished. The orange-green-orange colormap is applied to show desirable and undesirable velocity and pressure combinations. Note the minimal separation at all velocities for zero backfill pressure.

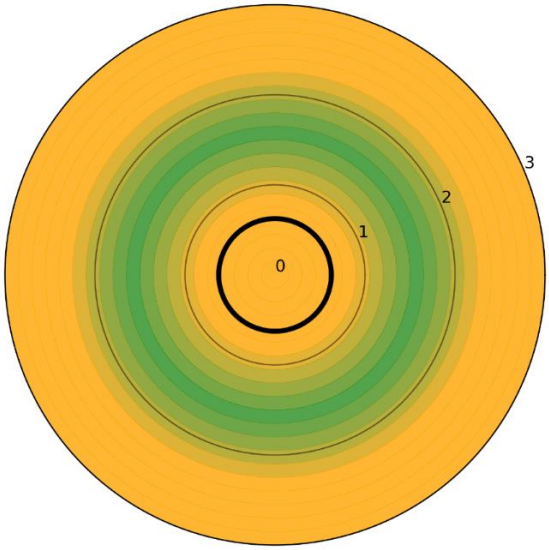

Figure 3.2. The same colormap displayed on the sabot stripper plate. The inner bolded circle demarcates the hole in which the projectile travels through. The radial ticks denote the radis in inches.

A 2D contour plot is a more suitable method of examining the degree of separation in relation to the regressors. Figures 3.3 and 3.4 distinguish between the 4 mm and 10 mm sabot geometry. As the velocity approaches the higher end of the range, the degree of separation appears to become increasingly independent of velocity. This occurrence appears to intensify with a lower backfill pressure. A lack of separation time is a possible explanation. As the velocity increases, the sabot has less time to travel the fixed distance to the sabot stripper plate. When the sabot rotates during separation, more projected area is exposed to the freestream velocity, producing a relationship of increased rate of separation with increased separation. Logically, the sabot will experience the most separation at a time later in its flight. If the travel time is decreased, the sabot cannot achieve the state of increased separation. The effects of this incidence at least partially negate the increased separation due to higher aerodynamic forces at increased velocities.

Sabot data points for each geometry are plotted on their respective contours. Additionally, occurrences of sabot failure are plotted on the contours. It is important to note that these failure data points are not used in the polynomial regression model, due to no associated degree of separation data available. Examining the diagnostic videos taken by the HVIL's high-speed camera, sabot failure is determined if a significant portion of the sabot enters the target tank with the projectile. These failure data points, in combination with the minimum successful data points used in polynomial regression, are used to develop loci for states of failure from aerodynamic breakup (top dashed line) or inadequate separation (bottom dashed line). A lack of available testing in proximity to these loci presents a limitation to the accuracy in these regions.

The plotted data indicates aerodynamic breakup is less likely when high backfill pressures are applied to lower velocities. Testing experience also conveys a lower risk of

aerodynamic heating in this range. At lower velocities, the sabot can be separated to a much greater degree with little to no complication. Expanding the possible degree of separation to cover the more stripper plate area increases its operational lifetime. The sabot stripper life optimization curve is plotted on the contour. The curve is formulated using the logistic function applied to the top and bottom failure loci. The logistic function including the parameters used is shown in Equation 2.1. The midpoint of the function is 4500 meters per second, the mean of the operational range used in the regression. The logistic growth rate is 0.000694, resulting in a logistic constant of 85% at a velocity of 7000 meters per second and a constant of 15% at a 2000 meters per second. For example, at 7000 meters per second, the optimization curve is formulated with 85% of the bottom failure locus and 15% of the top. Finally, an offset of 250 meters per second is applied to the optimization curve. The failure loci and optimization curves are formulated with experimental data but are tailored to the HVIL's 2SLGG to improve performance. It is unlikely that the curves can be accurately externalized to other experimental setups.

$$f(V) = \frac{1}{1 + e^{-0.000694(V-4500)}} \tag{3.1}$$

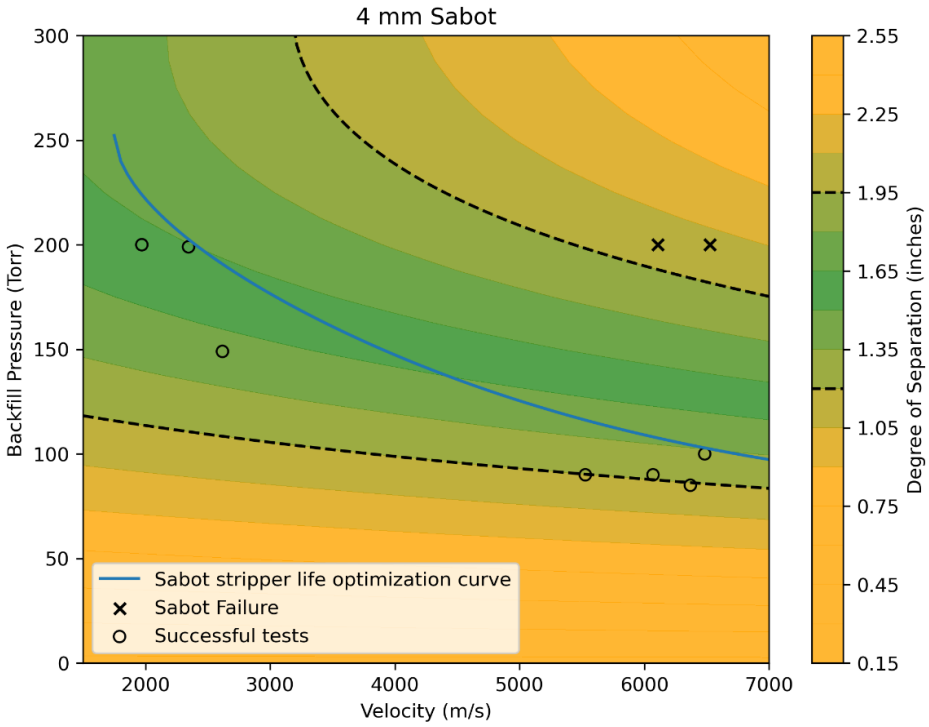

Figure 3.3. 2D surface demonstrating the degree of separation of a 4 mm sabot as a function of the projectile velocity and backfill pressure. The failure loci (dashed lines) are also plotted on the colorbar for reference.

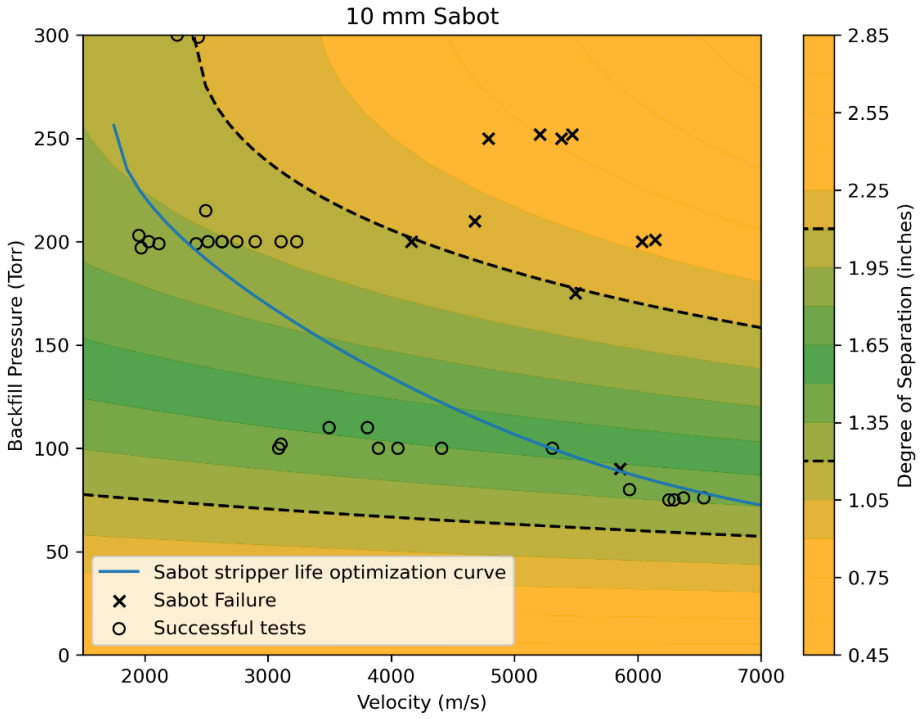

Figure 3.4. 2D surface demonstrating the degree of separation of a 10 mm sabot as a function of the projectile velocity and backfill pressure.

The results of the circularity investigation are shown in Figure 3.5. Velocity significantly correlates with the average impact contour circularity. Possible explanations for systematic errors leading to a lower R square value of 0.38 include human tracing error of impact contours and interactions between impacting sabot petals and existing impact deformations. Often, the impact of a sabot will be augmented by nearby deformations. The decreased initial impact resistance of a nearby crater will guide the sabot petal in that direction as it impacts. Additionally, crater edge material is strain hardened by previous impact and will not deform as easily as non-cratered surface, effectively artificially bounding the impact zone. Increasing roundness is associated with increasing compactness of impact; at a given velocity, a rounder impact signals the sabot did not rotate enough to impact the stripper plate broadside. Less round impacts indicate the sabot achieved sufficient rotation to impact the longitudinal face of the petal into the stripper plate. Experimental evidence indicates a more circular resultant impact contour is associated with an increase in stripper plate deformation. Therefore, a less circular impact is desirable as it distributes the transfer of kinetic energy over a larger area and decreases local impact stress. For a given velocity, backfill pressure parameters generally resulting in a less round impact can improve sabot stripper life. More investigation is needed to determine the extent and characteristics of such a pattern.

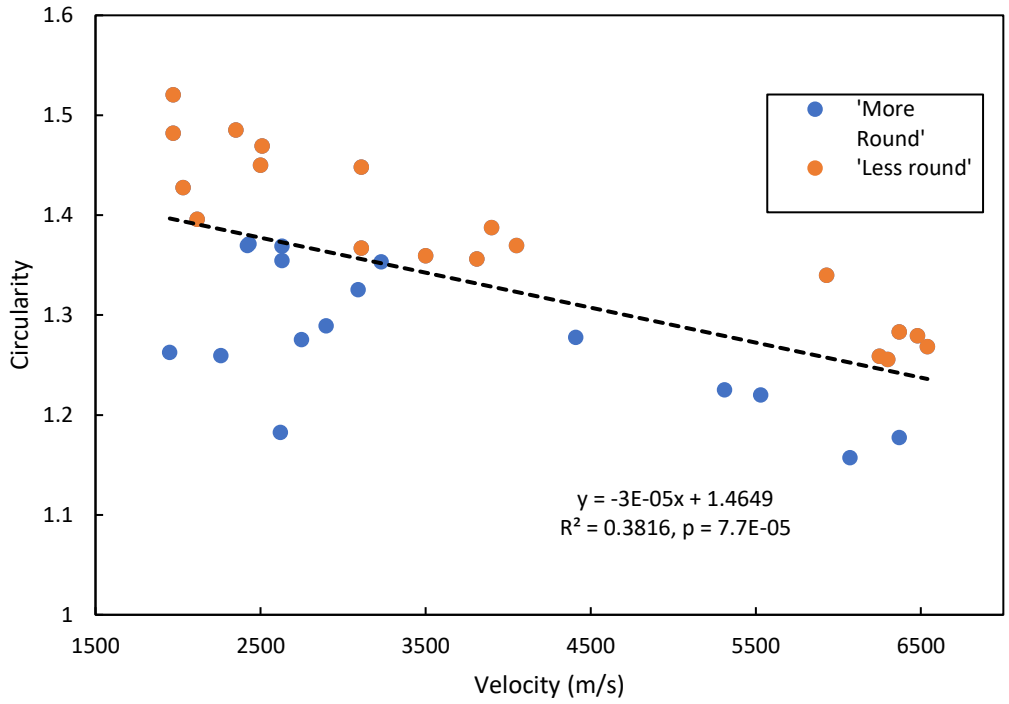

Figure 3.5. Impact contour circularity as a function of velocity for the 35 collected data points. Linear regression yields a statistically significant relationship. The desirable 'less round' data points are denoted as being above the trendline for a given velocity.

4. CONCLUSION

An empirical model to describe the degree of sabot separation during hypervelocity testing was developed using polynomial regression. The sabot stripper plate was photographed post-impact for 35 hypervelocity impact tests through conducted in the Texas A&M University Hypervelocity Impact Laboratory. Sabot impact locations in the image data were converted into the radial distance, or the degree of separation, from the projectile's nominal flight trajectory using the image processing library OpenCV in Python. Utilizing aerodynamic laws and previous testing data, a polynomial regression model was formulated using launch parameters such as projectile velocity and blast tank backfill pressure. The model also accounted for the different sabot geometry required to launch 4 mm and 10 mm spherical projectiles.

The polynomial regression model (N = 36) was found to describe the degree of separation with an R square value of 0.92 and a standard error of 0.1 inches. All regressors were found to be statistically significant at the $p = 0.01$ level. The model was mapped onto a 2D contour surface for additional analysis and in situ testing reference. Successful test data used for the regression model was added to the plot. Known sabot failures through aerodynamic breakup were also plotted; this data was not used in the regression model. The plotting of these points allowed for the qualitative generation of failure loci. Additional analysis revealed an ideal curve combining velocity and pressure launch parameters to maximize sabot separation success in testing and sabot stripper plate operational life.

Accurately predicting the degree of sabot separation is crucial to reducing testing turnaround time and consumable use. Qualitatively relating launch parameters to the resulting sabot separation is externalizable, even with different launch configurations. Empirically

modelling 2-stage light gas gun behavior is invaluable for the development of new hypervelocity testing facilities.

Future investigative work will focus on empirically modeling aspects of sabot rotation to lengthen the sabot stripper plate's operational life. A more thorough future investigation into the scalable aspects of the empirical model developed in this study will determine the extent in which the studied sabot behavior can be applied in similitude models to evaluate testing configurations for higher projectile velocity and mass regimes.

REFERENCES

[1] Sayler, K., 2020, Hypersonic Weapons: Background and Issues for Congress, Congressional Research Service, pp. 9-22. https://fas.org/sgp/crs/weapons/R45811.pdf.

[2] 1991, Critical technologies for national defense, American Institute of Aeronautics and Astronautics, Washington, DC.

[3] Schonberg, W. P., "Studies of hypervelocity impact phenomena as applied to the protection of spacecraft operating in the MMOD environment," Procedia Engineering, Vol. 204, 2017, pp. 4–42. https://doi.org/10.1016/j.proeng.2017.09.723.

[4] Schonberg, W. P., "Hypervelocity Impact Penetration Phenomena in Aluminum Space Structures," Journal of Aerospace Engineering, Vol. 3, No. 3, 1990, pp. 173–185. https://doi.org/10.1061/(ASCE)0893-1321(1990)3:3(173).

[5] Schonberg, W. P., "Protecting spacecraft against meteoroid/orbital debris impact damage: an overview," Tech. rep., 2001.

[6] Christiansen, E., "Micrometeoroid and Orbital Debris (MMOD) Risk Overview," 2014. https://doi.org/https://ntrs.nasa.gov/ archive/nasa/casi.ntrs.nasa.gov/20140009950.pdf.

[7] Grosch, D. J., and Riegel, J. P., 1993, "Development and optimization of a "micro" two-stage light-gas gun", International Journal of Impact Engineering, **14**(1-4), pp. 315–324.

[8] Berggren, R. E. and R. M. Reynolds, 1970. The Light-Gas-Gun Model Launcher. AGARDograph No. 138 on Ballistic Range Technology, pp. 99-119.

[9] Swift, H.F., and Strange, D.E., 1987, "Sabot Discard Technology", Internal papers - Physics Applications Inc., pp. 1-10.

[10] Jacob Rogers, Paul T. Mead, Khari Harrison, Kalyan Raj Kota, James D. Leaverton, Gavin Lukasik, Waruna D. Kulatilaka, Justin W. Wilkerson and Thomas E. Lacy. "Hypervelocity Impact Response of Polyethylene Plates," AIAA 2021-0887. AIAA Scitech 2021 Forum. January 2021.